ELSEVIER

Biophysical Chemistry 122 (2006) 136–142

Biophysical Chemistry

http://www.elsevier.com/locate/biophyschem

Dielectric properties of *E. coli* cell as simulated by the three-shell spheroidal model

Wei Bai [a], K.S. Zhao [a,*], K. Asami [b]

[a] *Department of Chemistry, Beijing Normal University, 100875, Beijing, China*
[b] *Institute for Chemical Research, Kyoto University, Uji, Kyoto 611-0011, Japan*

Received 6 November 2005; received in revised form 12 March 2006; accepted 12 March 2006
Available online 16 March 2006

Abstract

Dielectric properties of *E. coli* cell have been re-studied by means of the three-shell spheroidal model, where the three shells correspond to the outer membrane, the periplasmic space and the inner membrane, respectively. With the model, a curve-fitting procedure has been developed to analyze the dielectric spectra. Although *E. coli* cell has been studied before, its special morphological structure was taken into account more comprehensively than any previous model in the present work. Dielectric properties of various cell components have been estimated from the observed dielectric spectra, especially the permittivity of the outer membrane, which was evaluated quantitatively for the first time. The values of ε_{om} were 12 for κ_{om} of 0 to 10^{-4} S/m and 34 for κ_{om} of 10^{-3} S/m. The specific capacitance of the inner membrane was 0.6–0.70 μF/cm^2. The relative permittivity and the conductivity of the cytoplasm were about 100 and 0.22 S/m, respectively, and the conductivity of the periplasmic space was 2.2–3.2 S/m.

Keywords: Dielectric spectroscopy; *E. coli*; Electric cell model; Interfacial polarization; Membrane capacitance; Conductivity

1. Introduction

With the rapid development of dielectric spectroscopy and AC electrokinetic methods, various biological cells and supramoleculars have been studied since the beginning of the 20th century [1–13]. *E. coli* cell was always an attractive subject in this field. The cell suspensions show dielectric relaxation due to interfacial polarization in the radio frequency range. Analysis of the dielectric relaxation is seriously dependent on the electric models of the cells, and therefore various electric models have been proposed. Fricke [14–16] firstly applied the one-shell spherical model for estimating the membrane capacitance and the cytoplasmic conductivity. However, his theory was insufficient both to estimate the electric parameters of the other cellular components and to predict the frequency-dependence of the conductivity and permittivity of the cell suspensions. Carstensen et al. [17] proposed a two-shell spherical model that included an outer conducting shell corresponding to the cell wall, in order to explain the abnormally high conductivity of bacterial suspensions, which was observed with dilute electrolyte solutions at low frequencies.

Asami et al. [18] developed a theory based on a two-shell spheroidal model for *E. coli* cells, in which the two shells corresponded to the plasma membrane and the relatively thicker cell wall. However, there was still some discrepancy between the observed and the theoretical dielectric spectra. They interpreted the discrepancy in terms of dielectric relaxation in the cytoplasm.

Recently, Hölzel [19] studied dielectric properties of *E. coli* cells by means of electrorotation, and estimated the electric parameters of the cellular components using a three-shell spherical model that had the periplasmic space between the outer and the inner membranes. For Gram-negative bacteria, the three-shell spherical model is more realistic than previous ones

* Corresponding author. Tel.: +86 10 58808283.
E-mail address: zhaoks@bnu.edu.cn (K.S. Zhao).

0301-4622/$ - see front matter © 2006 Elsevier B.V. All rights reserved.
doi:10.1016/j.bpc.2006.03.004

in view of their morphological structure [20,21], but it is not suitable for *E. coli* cells of rod-shape.

In this study, we analyzed the dielectric spectra exhibited by *E. coli* cell suspensions by means of a three-shell spheroidal model and estimated the electric properties of more cell components, such as the permittivity of the outer membrane and the conductivity of the periplasmic space. Further, we attempt to account for the discrepancy between the observed and the theoretical spectra with the two-shell spheroidal model pointed out by Asami et al. [18].

2. Electric model of *E. coli* cell

E. coli cells are of rod-shape, and their envelope consists of the outer and inner membranes separated by the periplasmic space of about 10 nm in thickness. The fundamental structure of the inner membrane is a lipid bilayer like other cellular membranes. The outer membrane, unlike the inner membrane, is principally made of an outer leaflet of lipopolysaccharides and an inner leaflet of phospholipids. The periplasmic space includes peptidoglycan that is the main component of the bacterial cell wall [20,21]. Since the three layers have different electric properties, a spheroidal model with three shells may be suited for *E. coli* cells (Fig. 1). This model is an extension of the spheroidal model with two confocal shells described in a previous paper [18]. The symbols used in the model are listed in Appendix.

According to the Maxwell–Wagner interfacial polarization theory, when the shell-covered ellipsoids are randomly dispersed in a continuous medium of complex relative permittivity ε_a^* at volume fraction P ($P<0.1$), the complex relative permittivity ε^* of the suspension is given by

$$\varepsilon^* = \varepsilon_a^* \frac{\frac{2}{9}P\sum_{k=x,y,z}\frac{\varepsilon_{pk}^*-\varepsilon_a^*}{\alpha_k\varepsilon_{pk}^*+(1-\alpha_k)\varepsilon_a^*}+1}{1-\frac{1}{9}P\sum_{k=x,y,z}\frac{\varepsilon_{pk}^*-\varepsilon_a^*}{\alpha_k\varepsilon_{pk}^*+(1-\alpha_k)\varepsilon_a^*}} \tag{1}$$

The detailed derivation of Eq. (1) should be referred to the literature [11,18,22]. The equivalent complex relative permittivity ε_{pk}^* of the shell-covered ellipsoid along k-axis ($k=x,y,z$) is represented as

$$\varepsilon_{pk}^* = \varepsilon_{om}^* \frac{\beta_k(1-v_1)\varepsilon_{om}^* + (1+\beta_k v_1)\varepsilon_{qk}^*}{(\beta_k+v_1)\varepsilon_{om}^* + (1-v_1)\varepsilon_{qk}^*} \tag{2}$$

with

$$\varepsilon_{qk}^* = \varepsilon_{pp}^* \frac{\beta_k(1-v_2)\varepsilon_{pp}^* + (1+\beta_k v_2)\varepsilon_{mk}^*}{(\beta_k+v_2)\varepsilon_{pp}^* + (1-v_2)\varepsilon_{mk}^*}, \tag{3}$$

$$\varepsilon_{mk}^* = \varepsilon_{im}^* \frac{\beta_k(1-v_3)\varepsilon_{im}^* + (1+\beta_k v_3)\varepsilon_{cp}^*}{(\beta_k+v_3)\varepsilon_{im}^* + (1-v_3)\varepsilon_{cp}^*}, \tag{4}$$

$$\beta_k = (1-\alpha_k)/\alpha_k. \tag{5}$$

The depolarization factors α_x, α_y, α_z along the x-, y- and z-axes for prolate spheroids ($R_z>R_x=R_y$) are given by

$$\alpha_z = -\frac{1}{q^2-1} + \frac{q}{(q^2-1)^{3/2}}\ln\{q+(q^2-1)^{1/2}\}, \tag{6}$$

$$\alpha_x = \alpha_y = \frac{1}{2}(1-\alpha_z), \tag{7}$$

where q is the axial ratio defined as $q=R_z/R_x$. The volume ratios v_1, v_2 and v_3 were approximately written as:

$$v_1 = \frac{(R_z-d_{om})(R_x-d_{om})^2}{R_z R_x^2}, \tag{8}$$

$$v_2 = \frac{(R_z-d_{om}-d_{pp})(R_x-d_{om}-d_{pp})^2}{(R_z-d_{om})(R_x-d_{om})^2}, \tag{9}$$

$$v_3 = \frac{(R_z-d_{om}-d_{pp}-d_{im})(R_x-d_{om}-d_{pp}-d_{im})^2}{(R_z-d_{om}-d_{pp})(R_x-d_{om}-d_{pp})^2}. \tag{10}$$

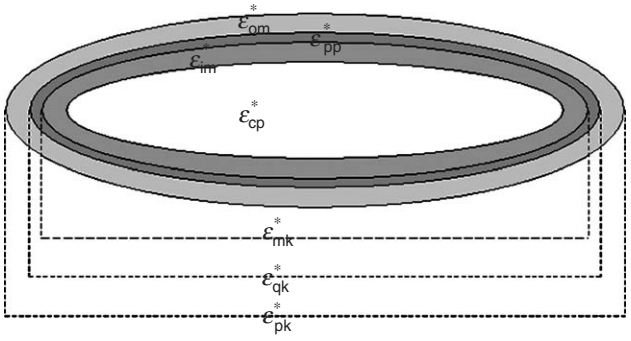

Fig. 1. The three-shell spheroidal model for *E. coli* cell. The surfaces of the three shells are represented by a family of confocal ellipsoids. For the symbols in the figure, see List of Symbols.

Since the derivation of these equations is similar to that described in previous papers, for details of the derivation, Refs. [11,18,22] should be referred to.

Although, in the three-shell model represented by a family of confocal ellipsoids, the thickness of each shell is non-uniform, we assumed uniform shell thicknesses d_{om}, d_{pp} and d_{im} because d_{om}, d_{pp}, $d_{im} \ll R_x$, R_y. We assumed a prolate spheroid for rod-shaped *E. coli* cells, which may not cause serious errors in estimation of the electric parameter of the cellular components from the observed dielectric spectra. Sekine et al. [23] numerically calculated the dielectric spectra for the rod-shaped model and compared with those for the prolate-spheroidal model. They concluded that there was no considerable difference between them.

3. Materials and methods

3.1. Preparation of E. coli cell suspensions

E. coli cells (K 12) were grown in shaken cultures in Luria–Bertani(LB) culture medium at 37 °C and were harvested in the stationary growth phase. The culture medium containing 10 g tryptone, 5 g yeast extract and 10 g NaCl per liter was adjusted to pH 7.0. The culture medium was sterilized before inoculation, and all operations before dielectric measurement were carried out in the sterile environment. The harvested cells were washed twice with a 30 mM NaCl solution. The cell suspension was then allowed to stand for 1 h so as to equilibrate the cells in the suspending medium (i.e. 30 mM NaCl solution). Before dielectric measurement the cells were again washed with the same suspending medium. The dimensions of cells were determined with about 150 cells by measuring them under a phase contrast microscope.

3.2. Dielectric measurements

Dielectric measurements were carried out for cell suspensions over a frequency range of 1 kHz to 110 MHz with a 4294A Precision Impedance Analyzer with a 16047E Spring Clip fixture (Agilent Technologies). The measuring cell used was a parallel plate capacitor consisting of two platinized platinum plates and a lucite spacer, cell constant and sample space being 0.02 pF and 200 μl, respectively. The details of the measuring cell were described in a previous paper [24]. After the measurement of cell suspensions, the suspending medium was immediately separated by centrifugation to measure its relative permittivity and conductivity. All measurements were performed at 21 ± 1 °C.

The raw data measured by the impedance analyzer were corrected for residual inductance and stray capacitance arising from the measuring cell and its fixture by the method described in a previous paper [25]. At lower frequencies, a marked electrode polarization effect dominates, owing to the counterion accumulation at the electrode-aqueous phase interface. And in the present paper the correction procedure proposed by Raicu et al. was employed to eliminate the artefact, which can eliminate the real and imaginary part of electrode polarization simultaneously [26].

3.3. The curve-fitting procedure based on the three-shell spheroidal model

To estimate the dielectric phase parameters of *E. coli* cells from the experimental dielectric spectra, a curve-fitting procedure was established on the basis of examination of the responses of dielectric spectra to changes in each parameters. In Fig. 2 are shown eight sets of theoretical curves obtained by changing one of the phase parameters P, ε_{om}, ε_{cp}, ε_{im}, κ_{pp}, κ_{cp},κ_{im} and κ_{om}. The responses of dielectric spectra are summarized as follows:

(1) The limiting conductivity at low frequency κ_l decreases as the volume fraction P increases, and increases with κ_{om}.
(2) The limiting relative permittivity at low frequency ε_l is sensitive to P, ε_{om} and κ_{om}.
(3) The limiting relative permittivity at high frequency ε_h increases with ε_{cp}.
(4) The relative permittivity in the middle of the dielectric relaxation ε_m decreases with ε_{im}.
(5) The shape of dielectric relaxation between 0.5 and 5 MHz is dependent on κ_{pp}.
(6) The shape of dielectric relaxation between 5 and 100 MHz is mainly related to κ_{cp}.

On the basis of the effects of the individual phase parameters on dielectric relaxation as summarized above, a curve-fitting procedure can be obtained for determination of the phase parameters as follows:

Step 1. Put temporarily phase parameters as $\kappa_{pp}=\kappa_{cp}=\kappa_a$, $\varepsilon_{im}=\varepsilon_{om}=6$, $\varepsilon_{cp}=\varepsilon_a=60$, $\varepsilon_{pp}=60$. The conductivity of the inner membrane κ_{im} is assumed to be 0 S/m, which is reasonable for ordinary plasma membranes. Since the structural and ion permeability properties of the outer membrane are different from those of the inner membrane, we fixed its conductivity value (κ_{om}) between 0 and 10^{-3} S/m (corresponds to a specific membrane resistance of about 0.1 Ω cm^2).
Step 2. Search P so as to fit the calculated κ_l to the observed κ_l.
Step 3. Search ε_{om}, so as to fit the calculated ε_l to the observed ε_l.
Step 4. Search ε_{cp} so as to fit the calculated ε_h to the observed ε_h.
Step 5. Search ε_{im} so as to fit the calculated ε_m to the observed ε_m.
Step 6. Search κ_{pp} so as to fit the theoretical values to the observed ones between 0.5 MHz and 5 MHz.
Step 7. Search κ_{cp} so as to fit the theoretical values to the observed ones between 5 and 100 MHz.

In general, following the above fitting order, the steps (especially from Steps 3–7) were carried out repeatedly until the theoretical curve could agree well with the experimental data. This similar method has been adopted by many researchers [18,22,27,28]. To obtain the best-fit parameters, the residuals between theoretical curves and experiment data were minimized by means of a computer.

$$\mathrm{Dev}(\varepsilon,\kappa)=\left(\sum_i(\varepsilon_{ti}-\varepsilon_{ei})^2\Big/\sum_i\varepsilon_{ei}^2+\sum_i(\kappa_{ti}-\kappa_{ei})^2\Big/\sum_i\kappa_{ei}^2\right)^{1/2}$$

where ε and κ are permittivity and conductivity of the cell suspensions, and subscripts ti and ei stand for theoretical and experimental values at ith frequency, respectively.

4. Results

Fig. 3 shows a typical dielectric spectrum obtained in measurements on *E. coli* cells suspensions, which is due to the

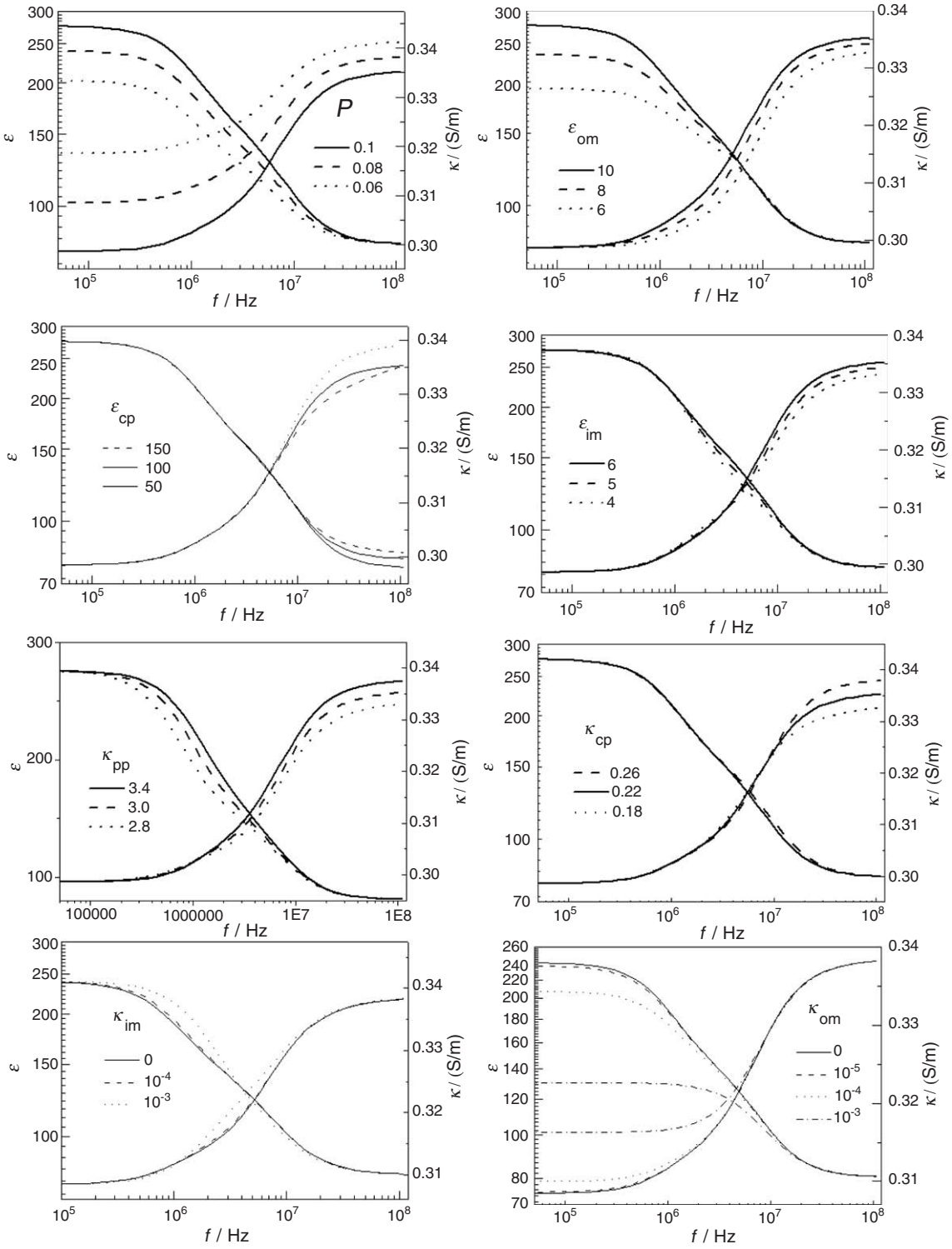

Fig. 2. The effects of the dielectric phase parameters P, ε_{om}, ε_{cp}, ε_{im}, κ_{pp}, κ_{cp},κ_{im} and κ_{om} on dielectric relaxation, assessed with the three-shell spheroidal model. The reference values: ε_a=81, κ_a=0.35 S/m, ε_{om}=10, κ_{om}=0, ε_{pp}=60, κ_{pp}=3 S/m, ε_{im}=6, κ_{im}=0, ε_{cp}=100, κ_{cp}=0.22 S/m, R_z=2 μm, R_x=R_y=0.5 μm, d_{om}=d_{im}=0.007 μm, d_{pp}=0.01 μm, P=0.1.

interfacial polarization. The steep rise of permittivity at low frequencies was due to the electrode polarization, and was corrected as description in Section 3.2. A simple application of the two-shell ellipsoid model seemed not to account for the dielectric behavior as pointed out by Asami et al. [18]. The discrepancy between the theoretical and experimental curves, however, has been satisfactorily overcome using the three-shell spheroidal model in this paper. As clearly seen in Fig. 3, the agreement between the theoretical and experimental curves is satisfactory over the entire dielectric spectra except the

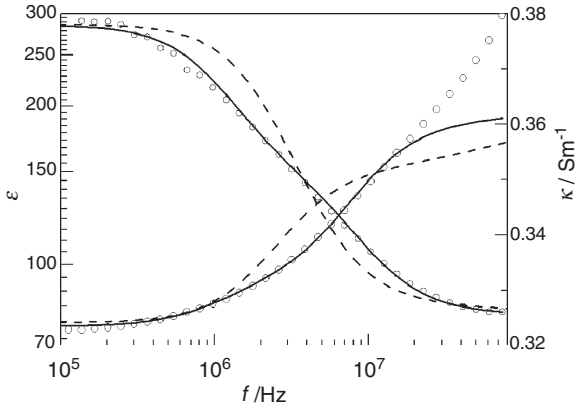

Fig. 3. Dielectric dispersion curves for *E. coli* cell suspension. The circles are the observed data. The solid lines are the theoretical curves calculated with the three-shell spheroidal model; here only curves for $\kappa_{om}=0$ are shown. The broken lines are the theoretical curves calculated with the two-shell spheroidal model.

conductivity at high frequencies above 20 MHz, where it was possibly because the conductivity data above 20 MHz may include instrumental or uncorrected errors and the contributions of molecular relaxation in the cells. The curve-fittings have been performed by fixing the conductivity of the outer membrane between 0 and 10^{-3} S/m considering its high permeability to ions. Table 1 summarizes the best-fit phase parameters obtained for eight different experiments. The estimated phase parameters were almost independent of κ_{om} of up to 10^{-4} S/m, and for κ_{om} of 10^{-3} S/m the values of P and ε_{om} considerably changed whereas the other phase parameters were almost unchanged. In addition, we examined the changes of the phase parameters by changing periplasm thickness from 10 to 15 nm when $\kappa_{om}=10^{-3}$ S/m and other morphological parameters being held constant. The results showed that the conductivity of the periplasmic space reduced from 3.3±0.2 to 2.2±0.2 S/m, while other derived phase parameters were almost unchanged.

5. Discussion

The present study demonstrated that the three-shell spheroidal model provided better simulations for dielectric spectra of *E. coli* cell suspensions. The agreement between the theoretical and observed curves was satisfactory, which has never been obtained by the two-shell spheroidal model. Thus, the estimation of the electric parameters of cell components would be more reliable with the three-shell spheroidal model than the other previous models.

With the three-shell spheroidal model, there are many variables so that conventional curve fitting algorithms are not simply applicable to the observed dielectric spectra. Hence, to establish the curve fitting procedure, we examined the effects of the electrical phase parameters on the dielectric spectra. Some of the parameters were found to be of less influence on the dielectric spectra and therefore were appropriately fixed to reduce the number of variables. We carefully chose the fixed morphological and electrical parameters by reference to previous studies [29,30]. Such curve fitting procedure has been successfully used with various models [10,11, and references therein].

For *E. coli* cell, the outer membrane is considered to have much higher conductivity than the ordinary plasma membranes, because it contains a number of channels called porins through which small ions and molecules such as glucose can considerably permeate [31–33]. Unfortunately, no quantitative value of its conductivity has been reported so far. Therefore, in order to reduce the number of unknown parameters, we had to fix the value of κ_{om} between 0 and 10^{-3} S/m (corresponds to a specific membrane resistance of about 0.1 Ω cm^2) to determine other phase parameters. As a result of the curve fitting, all phase parameters estimated were almost independent of $\kappa_{om}\leq 10^{-3}$ S/m except ε_{om}. Accuracies of these parameters were limited within 10%.

The relative permittivity of the outer membrane was determined to be 10 to 12 for $\kappa_{om}\leq 10^{-4}$ S/m and 34 for $\kappa_{om}=10^{-3}$ S/m, which values respectively correspond to specific membrane capacitances of 1.3–1.5 and 4.3 μF/cm^2. These values are higher than those reported for the plasma membranes [1,7,12,27,34,35]. This may be related to the composition and structure of the outer membrane. The outer membrane is different from ordinary lipid bilayers found for the plasma membranes; it is made of an outer leaflet consisting of lipopolysaccharide and an inner leaflet consisting of phospholipids. In addition, the outer membrane is much more permeable to sugar and ions than the inner membrane, and is not regarded as a barrier for ions but as a filter to exclude large molecules. The outer membrane would be more hydrophilic and have higher polarity than the ordinary plasma membranes. It is, therefore, reasonable that the outer membrane has a high permittivity.

The specific capacitance of the inner membrane was found to be 0.70 μF cm^{-2}, which is smaller than 1.5 μF cm^{-2} reported by Hölzel [19] and 1.9 μF cm^{-2} by Asami et al. [18], being

Table 1
The comparison of the phase parameters estimated with the three-shell ellipsoidal model at various conductivities of the outer membrane

κ_{om} (S/m^{-1})	P	ε_{om}	ε_{im}	ε_{cp}	κ_{cp} (S/m^{-1})	κ_{pp} (S/m^{-1})
0	0.083±0.014	10.0±0.7	5.5±0.3	108±5	0.22±0.03	3.2±0.2
10^{-6}	0.083±0.014	10.0±0.7	5.5±0.3	108±5	0.22±0.03	3.2±0.2
10^{-5}	0.083±0.014	10.2±0.7	5.5±0.3	108±5	0.22±0.03	3.2±0.2
10^{-4}	0.085±0.014	12.1±0.8	5.5±0.3	108±5	0.22±0.03	3.2±0.2
10^{-3}	0.101±0.016	34±2	4.9±0.2	108±5	0.22±0.02	3.3±0.2

$\kappa_a=0.36\pm0.01$ S/m. The morphological parameters: $R_z=2$ μm, $R_x=R_y=0.5$ μm, $d_{om}=d_{im}=0.007$ μm and $d_{pp}=0.01$ μm. The assumed electric phase parameters: $\varepsilon_a=80$, $\varepsilon_{pp}=60$, $\kappa_{im}=0$ S/m. The values of d_{om}, d_{im} and d_{pp} referred to those in literatures [20,21]. These values are means±standard deviations of 8 sets of experimental data.

consistent with those of plasma membranes and lipid bilayers [1,27,34,36].

The relative permittivity of the cytoplasm was about 100, which is slightly higher than that of water. This is possibly because of low accuracy in determination of ε_{cp}, as discussed in the papers [29,30]. On the other hand, the higher value may be interpreted as below: the cytoplasm is not a pure electrolyte solution, but is a sol-like system in which some components (such as proteins, granules and DNAs) are dispersed in the electrolyte solution; and such system was a bit similar to the microemulsion, which has relatively higher apparent permittivity as a whole in general [37].

The conductivity of the cytoplasm was 0.22±0.02 S/m. The value was similar to those reported previously, i.e., 0.44±0.1 S/m obtained by electrorotation with the three-shell spherical model [19], and 0.17 and 0.36 S/m by dielectric spectroscopy with the two-shell spheroidal and the two-shell spherical models, respectively [18,38].

The conductivity of the periplasmic space was estimated to be 2.2–3.2 S/m, being ten times higher than the conductivity of the outer medium. This value was not so different from 4 to 11.8 S/m obtained for κ_a of 0.006–0.09 S/m by electrorotation [19]. The reason for higher conductivity than κ_a may because the periplasmic space is filled with peptidoglycan, which acts like ion-exchange resin and absorbs ions in the surrounding medium [38].

6. Conclusion

We have analyzed dielectric spectra of *E. coli* cell suspensions and have derived dielectric properties of various cell components by means of the three-shell spheroidal model, which took its peculiar morphological structure into account more comprehensively than any previous model. Here it is necessary to note that because complex morphologies led to a great number of variable parameters embodied in the electric model, which decreased the data accuracy to a certain extent. However, as an extension of the two-shell spheroidal model, the three-shell spheroidal model can provide much information for more cell components, such as the permittivity of the outer membrane and the conductivity of the periplasmic space. Probably, the accurate determination of dielectric properties might be restricted by other factors, and this would be improved in the future work.

Acknowledgement

This work is supported by the National Nature Science Foundation of China (No. 20273010).

Appendix A. List of symbols in three-shell spheroidal model

Morphological parameters

R_x, R_y, R_z The semi-axes of the outermost ellipsoid along x-, y-, z-axes, $R_z > R_x = R_y$

d_{om} The thickness of the outer membrane

d_{pp} The thickness of the periplasmic space

d_{im} The thickness of the inner membrane

Electric phase parameters

ε^* Complex relative permittivity defined as $\varepsilon^* = \varepsilon - j\kappa/\omega\varepsilon_0$

ε Relative permittivity

κ Conductivity

ω Angular frequency defined as $\omega = 2\pi f$, where f is frequency of ac field

ε_0 The permittivity of vacuum

ε^*_{om} The complex relative permittivity of the outer membrane, $\varepsilon^*_{om} = \varepsilon_{om} - j\kappa_{om}/\omega\varepsilon_0$

ε^*_{pp} The complex relative permittivity of the periplasm, $\varepsilon^*_{pp} = \varepsilon_{pp} - j\kappa_{pp}/\omega\varepsilon_0$

ε^*_{im} The complex relative permittivity of the inner membrane, $\varepsilon^*_{im} = \varepsilon_{im} - j\kappa_{im}/\omega\varepsilon_0$

ε^*_{cp} The complex relative permittivity of the cytoplasm, $\varepsilon^*_{cp} = \varepsilon_{cp} - j\kappa_{cp}/\omega\varepsilon_0$

ε^*_a The complex relative permittivity of the external medium, $\varepsilon^*_a = \varepsilon_a - j\kappa_a/\omega\varepsilon_0$

References

[1] H.P. Schwan, Electrical properties of tissue and cell suspensions, in: J.H. Lawrence, C.A. Tobias (Eds.), Advances in Biological and Medical Physics, vol. 5, Academic Press, New York, 1957, pp. 147–209.
[2] E.H. Grant, R.J. Sheppard, G.P. South, Dielectric Behavior of Biological Molecules in Solution, Oxford University Press, Oxford, 1978.
[3] R. Pethig, Dielectric and Electronic Properties of Biological Materials, Wiley, New York, 1979.
[4] U. Zimmermann, W.M. Arnold, The interpretation and use of the rotation of biological cells, in: H. Fröhlich, F. Kremer (Eds.), Coherent Excitations in Biological Systems, Springer-Verlag, Berlin, Heidelberg, 1983, pp. 211–221.
[5] S. Takashima, Electrical Properties of Biopolymers and Membranes, Adam Hilger, Bristol, 1989.
[6] T.B. Jones (Ed.), Electromechanics of Particles, Cambridge University Press, Cambridge, New York, Melbourne, 1995.
[7] R. Lisin, Ben-Zion Ginzburg, M. Schlesinger, Y. Feldman, Time domain dielectric spectroscopy study of human cells É erythrocytes and ghosts, Biochim. Biophys. Acta 1280 (1996) 34–40.
[8] E. Gheorghiu, K. Asami, Monitoring cell cycle by impedance spectroscopy: experimental and theoretical aspects, Bioelectrochem. Bioenerg. 45 (1998) 139–143.
[9] D.J. Bakewell, I. Ermolina, H. Morgan, J. Milner, Y. Feldman, Dielectric relaxation measurements of 12 kbp plasmid DNA, Biochim. Biophys. Acta 1493 (2000) 151–158.
[10] Jan Gimsa, Characterization of particles and biological cells by AC Electrokinetics, in: A.V. Delgado (Ed.), Interfacial Electrokinetics and Electrophoresis, Marcel Dekker Inc., New York, 2001, pp. 369–400.
[11] K. Asami, Characterization of heterogeneous systems by dielectric spectroscopy, Prog. Polym. Sci. 27 (2002) 1617–1659.
[12] F. Bordi, C. Cametti, T. Gili, Dielectric spectroscopy of erythrocyte cell suspensions. A comparison between Looyenga and Maxwell–Wagner–Hanai effective medium theory formulations, J. Non-Cryst. Solids 305 (2002) 278–284.
[13] A. Bonincontro, G. Onori, Investigation by dielectric spectroscopy of domain motions in lysozyme: effect of solvent and binding of inhibitors, Chem. Phys. Lett. 398 (2004) 260–263.
[14] H. Fricke, A mathematical treatment of the electric conductivity and capacity of disperse systems: I. The electric conductivity of a suspension of homogeneous spheroids, Phys. Rev. 24 (1924) 575–587.

[15] H. Fricke, A mathematical treatment of the electric conductivity and capacity of disperse systems: II. The capacity of a suspension of conducting spheroids surrounded by a non-conducting membrane for a current of low frequency, Phys. Rev. 26 (1925) 678–681.
[16] H. Fricke, H.P. Schwan, K. Li, V. Bryson, A dielectric study of the low-conductance surface membrane in *E. coli*, Nature (London) 177 (1956) 134–135.
[17] E.L. Carstensen, H.A. Cox, W.B. Mercer, L.A. Natale, Passive electrical properties of microorganisms: I. Conductivity of *Escherichia coli* and *Micrococcus lysodeikticus*, Biophys. J. (5) (1956) 289–300.
[18] K. Asami, T. Hanai, N. Koizumi, Dielectric analysis of *Escherichia coli* suspensions in the light of the theory of interfacial polarization, Biophys. J. 31 (1980) 215–228.
[19] R. Hölzel, Non-invasive determination of bacterial single cell properties by electrorotation, Biochim. Biophys. Acta (1450) (1999) 53–60.
[20] Reginald H. Garrett and Charles M. Grisham. Biochemistry, 2nd Edition, Saunders College Publishing, Harcourt Brace College Publishers, 1999, p. 32.
[21] J. Ingraham, K.B. Low, B. Magasanik, M. Schaechter, H.E. Umbarger, F. C. Neidhardt (Eds.), *Escherichia coli* and *Salmonella typhimurium*: Cellular and Molecular Biology, vol. 1, American Society for Microbiology, 1987.
[22] K. Asami, T. Hanai, N. Koizumi, Dielectric approach to suspensions of ellipsoidal particles covered with a shell in particular reference to biological cells, Jpn. J. Appl. Phys. 19 (1980) 359–365.
[23] K. Sekine, N. Torii, C. Kuroda, K. Asami, Calculation of dielectric spectra of suspensions of rod-shaped cells using boundary element method, Bioelectrochemistry 57 (2002) 83–87.
[24] K. Asami, Dielectric properties of protoplasm, plasma membrane and cell wall in yeast cells, Bull. Inst. Chem. Res., Kyoto Univ. 55 (4) (1977) 394–414.
[25] K. Asami, A. Irimajiri, T. Hanai, N. Shiraishi, K. Utsumi, Dielectric analysis of mitochondria isolated from rat liver I: swollen mitoplasts as simulated by a single-shell model, Biochim. Biophys. Acta 778 (1984) 559–569.
[26] V. Raicu, T. Saibara, A. Irimajiri, Dielectric properties of rat liver in vivo: a noninvasive approach using an open-ended coaxial probe at audio/radio frequencies, Bioelectrochem. Bioenerg. 47 (1998) 325–332.
[27] V. Raicu, G. Raicu, G. Turcu, Dielectric properties of yeast cells as simulated by the two-shell model, Biochim. Biophys. Acta 1274 (1996) 143–148.
[28] A. Irimajiri, T. Hanai, A. Inouye, A dielectric theory of "multi-stratified shell" model with its application to a lymphoma cell, J. Theor. Biol. 78 (1979) 251–269.
[29] A. Bonincontro, J. Gimsa, G. Risuleo, V. Rosa, Critical analysis of the impedance method for the evaluation of permittivity and conductivity of the plasma membrane, Membr. Cell Biol. 14 (2000) 129–135.
[30] C.M. Mihai, M. Mehedintu, E. Gheorghiu, The derivation of cellular properties from dielectric spectroscopy data, Bioelectrochem. Bioenerg. 40 (1996) 187–192.
[31] H. Nikaido, Outer membrane, in: F.C. Neidhardt, R. Curtiss III, J.L. Ingraham, E.C.C. Lin, K.B. Low, B. Magasanik, W.S. Reznikoff, M. Riley, M. Schaechter, H.E. Umbarger (Eds.), *Escherichia coli* and *Salmonella*: Cellular and Molecular Biology, edn 2, ASM Press, Washington DC, 1996, pp. 29–47.
[32] T. Nakae, H. Nikaido, Outer membrane as a diffusion barrier in *Salmonella typhimurium*, J. Biol. Chem. 250 (1975) 7359–7365.
[33] J.W. Costerton, J.M. Ingram, K.J. Cheng, Structure and function of the cell envelope of gram-negative bacteria, Bacteriol. Rev. 38 (1974) 87–110.
[34] K. Asami, Y. Takahashi, S. Takashima, Dielectric properties of mouse lymphocytes and erythrocytes, Biochim. Biophys. Acta 1010 (1989) 49–55.
[35] J. Gimsa, R. Glaser, G. Fuhr, in: W. Schütt, H. Klinkmann, I. Lamprecht, T. Wilson (Eds.), Physical Characterization of Biological Cells, Verlag Gesundheitt, Berlin, 1991, pp. 295–323.
[36] K. Asami, A. Irimajiri, Dielectric dispersion of a single spherical bilayer membrane in suspension, Biochim. Biophys. Acta 769 (1984) 370–376.
[37] Y. Feldman, N. Kozlovich, Ido. Nir, N. Garti, Dielectric spectroscopy of microemulsions, Colloids Surf., A Physicochem. Eng. Asp. 128 (1997) 47–61.
[38] E.L. Carstensen, Passive electrical properties of microorganisms: II. Resistance of the bacterial membrane, Biophys. J. 7 (1967) 493–503.